

# Dip in UHECR and Transition from Galactic to Extragalactic Cosmic Rays

Veniamin Berezinsky

*INFN, Laboratori Nazionali del Gran Sasso, 67010 Assergi (AQ), Italy*

## Abstract

The dip is a feature in the diffuse spectrum of UHE protons in energy range  $1 \times 10^{18} - 4 \times 10^{19}$  eV, which is caused by electron-positron pair production on CMB photons. Calculated for power-law generation spectrum with index  $\gamma_g = 2.7$ , the shape of the dip is confirmed with high accuracy by data of Akeno - AGASA, HiRes, Yakutsk and Fly's Eye detectors. The predicted shape of the dip is robust: it is valid for the rectilinear and diffusive propagation, for different discretenesses in the source distribution, for local source overdensity and deficit, for source inhomogeneities on scale  $\ell \lesssim 100$  Mpc etc. Below the characteristic energy  $E_c \approx 1 \times 10^{18}$  eV the spectrum of the dip flattens for both diffusive and rectilinear propagation, and more steep galactic spectrum becomes dominant at  $E < E_c$ . The energy of transition  $E_{tr} < E_c$  approximately coincides with the position of the second knee  $E_{2kn}$  observed in the cosmic ray spectrum. The critical energy  $E_c$  is determined by the energy  $E_{eq} = 2.3 \times 10^{18}$  eV, where adiabatic and pair-production energy losses are equal. Thus, position of the second knee is explained by proton energy losses on CMB photons.

## 1. Introduction

The nature of signal carriers of UHECR is not yet established. The most natural primary particles are extragalactic protons. Due to interaction with the CMB radiation the UHE protons from extragalactic sources are predicted to have a sharp steepening of energy spectrum, so called GZK cutoff [1].

There are two other signatures of extragalactic protons in the spectrum: dip and bump [2] - [5]. The dip is produced due to  $p + \gamma_{CMB} \rightarrow p + e^+ + e^-$  interaction. The bump is produced by pile-up protons which loose energy in the GZK cutoff. As was demonstrated in [3], the bump is clearly seen in the calculations for a single source at large redshift  $z$ , but it practically disappears in the diffuse spectrum, because individual peaks are located at different energies.

As it will be discussed in this paper, the dip is a reliable feature in the UHE proton spectrum (see also [6] - [9]). Being relatively faint feature, it is however clearly seen in the spectra observed by AGASA, Fly's Eye, HiRes and Yakutsk arrays (see [10] - [15] for the data). We argue here that it can be considered as the confirmed signature of interaction of extragalactic UHE protons with CMB.

The dip has low-energy and high-energy flattenings (see Fig 1.). The high-energy flattening at  $E_a \approx 1 \times 10^{19}$  eV reproduces the *ankle*, the feature well seen in the observational data. The low-energy flattening at  $E_c \approx 1 \times 10^{18}$  eV, seen for both rectilinear [6] and diffusive [16, 17, 18] propagation, is a natural place for transition from extragalactic to galactic component of cosmic rays. Somewhere below  $E_c$  the more steep galactic component must appear. Thus  $E_c$  describes the beginning of transition (if one follows it from high energy side) or the energy where this transition completes (if one moves from low to high energy). We shall demonstrate here (see also [18]) that  $E_c$

is connected with  $E_{\text{eq}} = 2.3 \times 10^{18}$  eV, where pair-production and adiabatic energy losses are equal. The visible transition from galactic to extragalactic cosmic rays occurs at  $E_{\text{tr}} < E_c$ , and this energy coincides well with position of the *second knee* (Akeno -  $6 \times 10^{17}$  eV, Fly's Eye -  $4 \times 10^{17}$  eV, HiRes -  $7 \times 10^{17}$  eV and Yakutsk -  $8 \times 10^{17}$  eV).

The transition from galactic to extragalactic cosmic rays at  $E_c \approx 1 \times 10^{18}$  implies the dominance of the proton composition of the observed cosmic rays at  $E \gtrsim 1 \times 10^{18}$  eV. While HiRes [19] HiRes-MIA [20] and Yakutsk [21] data support this prediction and Haverah-Park [14] data do not contradict it at  $E \gtrsim (1 - 2) \times 10^{18}$  eV, the Akeno [22] and Fly's Eye [12] data favour the mixed composition, dominated by heavy nuclei (for a review see [15] and [23]).

Below we shall analyze the features in UHE proton spectrum using basically two assumptions: the uniform distribution of the sources in the universe and the power-law generation spectrum. We do not consider the possible speculations, such as cosmological evolution of sources. Only in Section 4. we shall turn to model-dependent consideration.

## 2. The dip

The analysis of the dip is convenient to perform in terms of the *modification factor*. Modification factor is defined as a ratio of the spectrum  $J_p(E)$  with all energy losses taken into account, and unmodified spectrum  $J_p^{\text{unm}}$ , where only adiabatic energy losses (red shift) are included.

$$\eta(E) = \frac{J_p(E)}{J_p^{\text{unm}}(E)}. \quad (1)$$

Modification factor is less model-dependent quantity than the spectrum. In particular, it depends

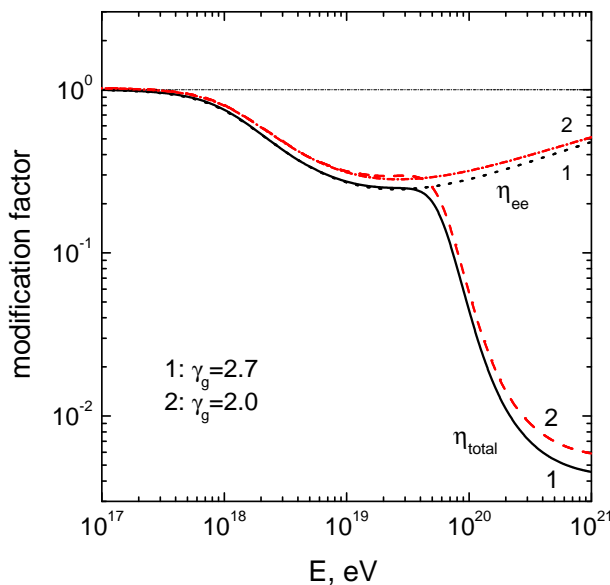


**Fig. 1.** Modification factor for the power-law generation spectra with  $\gamma_g$  in the range 2.0 - 2.7. Curve  $\eta = 1$  corresponds to adiabatic energy losses, curves  $\eta_{ee}$  - to adiabatic and pair production energy losses and curves  $\eta_{tot}$  - to total energy losses.

weakly on  $\gamma_g$ , because both numerator and denominator in Eq. (1) include  $E^{-\gamma_g}$ . In this paper we shall consider the non-evolutionary case  $m = 0$ . In Fig 1. the modification factors are shown as a function of energy for two spectrum indices  $\gamma_g = 2.0$  and  $\gamma_g = 2.7$ . They do not differ much.

Comparison of the predicted dip ( $\eta_{ee}$  curve) with observational data are shown in Fig 2. for  $\gamma_g = 2.7$ . One can observe the excellent agreement with AGASA, HiRes and Yakutsk data (and also with Fly's Eye data not presented here), while the Auger spectrum, at this preliminary stage, does not contradict the dip.

The systematic errors in energy determination of existing detectors exceed 20%. The dip can be used for energy calibration of detectors. Assuming the energy-independent systematic errors we shifted the energies of AGASA and HiRes by factor  $\lambda_{Ag} = 0.9$  and factor  $\lambda_{Hi} = 1.2$ , respectively, to reach the best fit of the dip. In Fig 3. the spectra of Akeno-AGASA and HiRes are shown before and after this energy calibration. One can see the good agreement of the data at  $E < 1 \times 10^{20}$  eV and their consistency at  $E > 1 \times 10^{20}$  eV. This result should be considered together with calculations [25], where it was demonstrated that 11 superGZK AGASA events can be simulated by the spectrum with GZK cutoff in case of 30% error in energy determination. We may tentatively conclude that existing discrepancy between AGASA, HiRes and Auger spectra at all energies may have statistical origin.

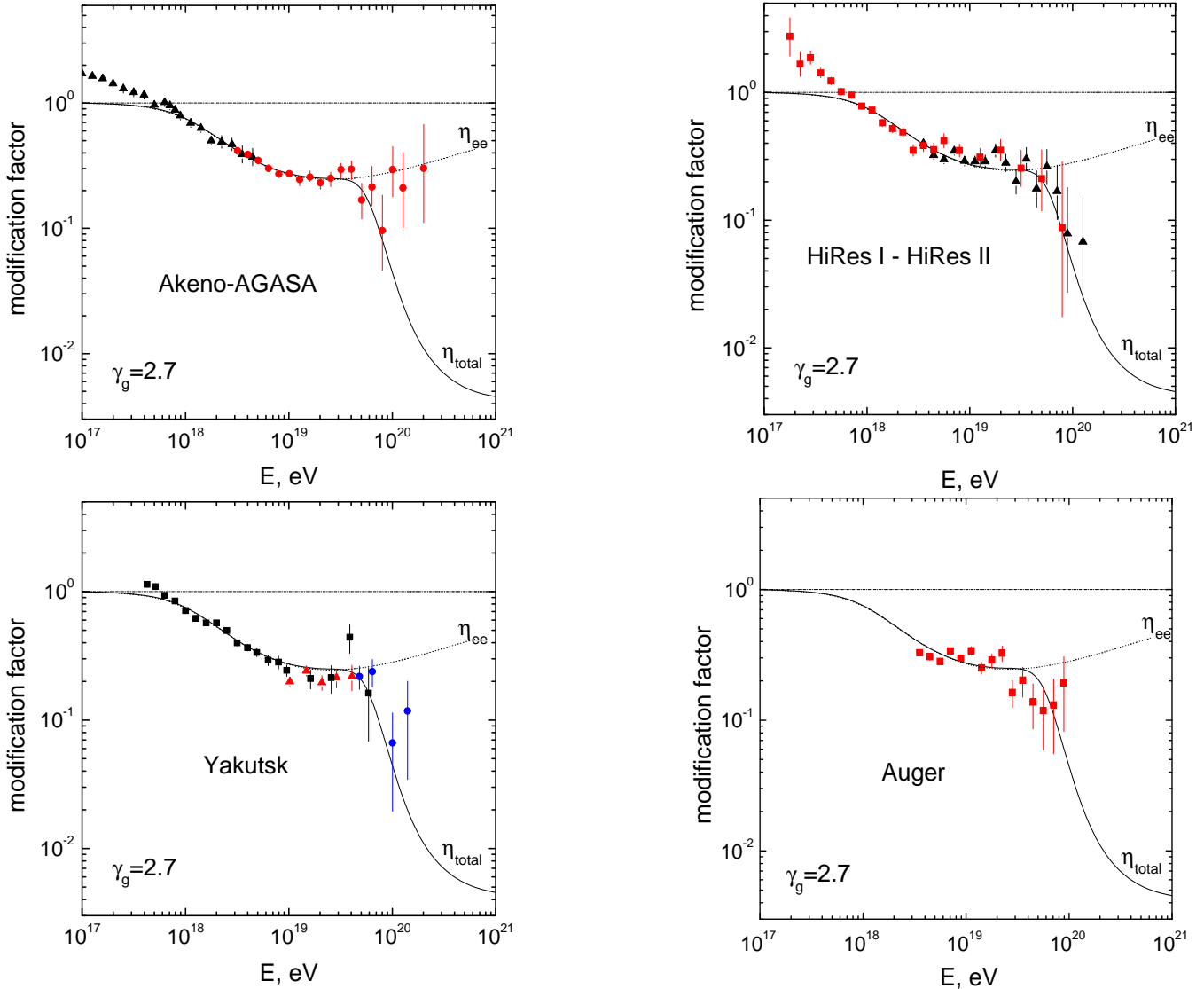


**Fig. 2.** Predicted dip in comparison with AGASA, HiRes, Yakutsk and Auger[24] data.

## 2.1 Robustness and caveats

How robust is prediction of the dip and what are uncertainties?

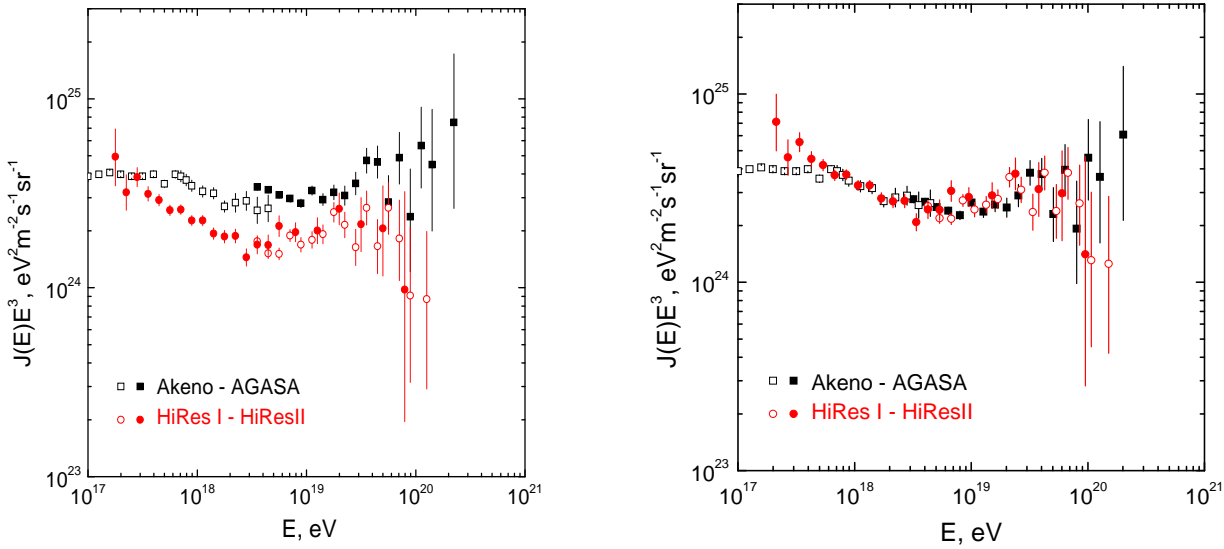


**Fig. 3.** Spectra of Akeno-AGASA and HiRes (left panel) and with energy calibrated by dip (right panel).

The shape of the calculated proton dip is stable relative to many phenomena included in calculations, namely, discreteness in the source distribution, mode of propagation (diffusive and rectilinear), inhomogeneities in source distribution on the scale  $\ell \lesssim 100$  Mpc, local source overdensity and deficit, acceleration  $E_{\max}$  and fluctuations in energy losses. However, it is modified by the assumption of source evolution [6] and by presence of UHE nuclei in primary flux [9] (see also [26]). In Fig 4. the dips for helium and iron nuclei are presented in comparison with the proton dip. One can see

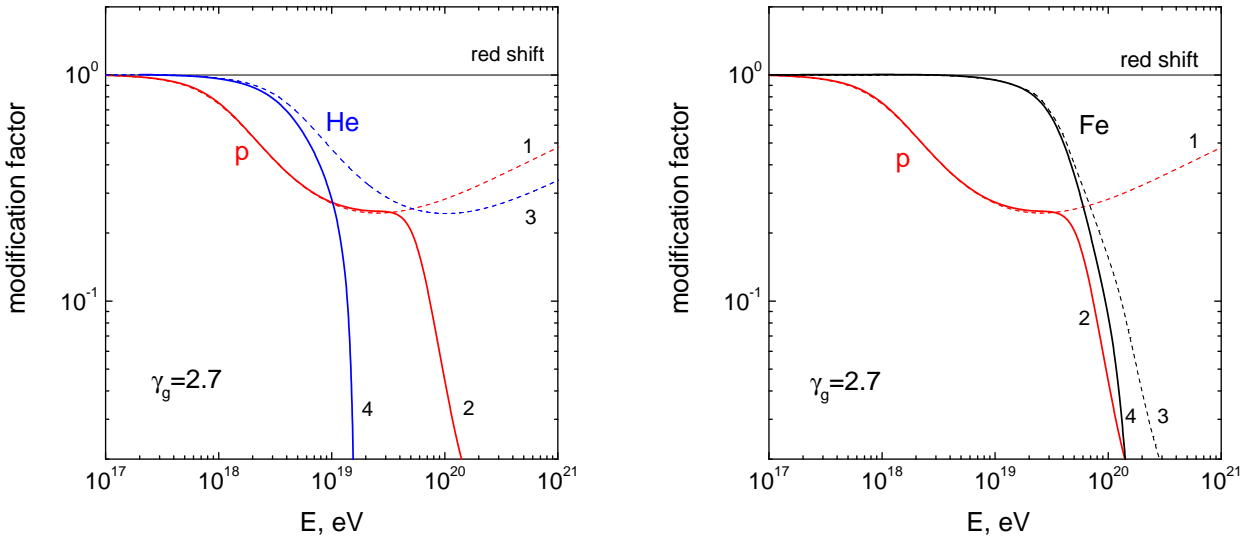


**Fig. 4.** Modification factors for helium and iron nuclei in comparison with that for protons. Proton modification factors are given by curves 1 and 2. Nuclei modification factors are given by curves 3 (adiabatic and pair production energy losses) and by curves 4 (with photodisintegration included).

that presence of 10 - 20 % of nuclei in the primary flux upsets the good agreement of proton dip with observations. Below we shall study this problem in a more detailed way.

Consider some acceleration mechanism operating in a gas with the mixed space density of hydrogen,  $n_H$ , and nuclei with atomic number  $A$ ,  $n_A$ . We assume the power-law generation spectrum

$$Q_A(p) = K_A n_A p^{-\gamma_g}, \quad (2)$$

where  $\gamma_g = 2.7$  and minimum momentum is  $p_A^{\min}$  for nuclei A. We assume also that the total number of particles accelerated per unit time  $Q_A^{\text{tot}} = Kn_A$ , where  $K$  is independent of  $A$  and of charge number  $Z$ . Then one obtains for the ratio of generation rates of  $A$  nuclei and protons

$$Q_A(p)/Q_p(p) = \begin{cases} (n_A/n_H)A^{\gamma_g-1} & \text{if } p_A^{\min} = v_{\min}\Gamma_{\min}Am_N \\ (n_A/n_H)Z^{\gamma_g-1} & \text{if } p_A^{\min} = R_{\min}Z \end{cases}, \quad (3)$$

where  $\Gamma$  is Lorentz factor and  $R = p/Z$  is rigidity. We shall refer to the upper case in Eq. (3) as to  $\Gamma$ -acceleration (it includes the shock acceleration) and to the lower case as to rigidity acceleration.

For rigidity acceleration in single-ionized gas,  $Z_{\text{eff}} = 1$ , one has

$$Q_A(p)/Q_p(p) = n_A/n_H \quad (4)$$

This ionization condition is important only near threshold of acceleration  $p \gtrsim p_A^{\min}$ , at higher energies the gas can be fully ionized

The modification factor for the mixed composition is given by

$$\eta(E) = \frac{\eta_p(E) + \lambda\eta_A(E)}{1 + \lambda}, \quad (5)$$

where  $\lambda = Q_A^{\text{unm}}(p)/Q_p^{\text{unm}}(p)$ . The strongest distortion of proton modification factor  $\eta_p(E)$  is given by helium nuclei for which  $n_A/n_H = 0.06$ , corresponding to mass ratio  $Y_p = 0.24$ . Fig 5. shows that

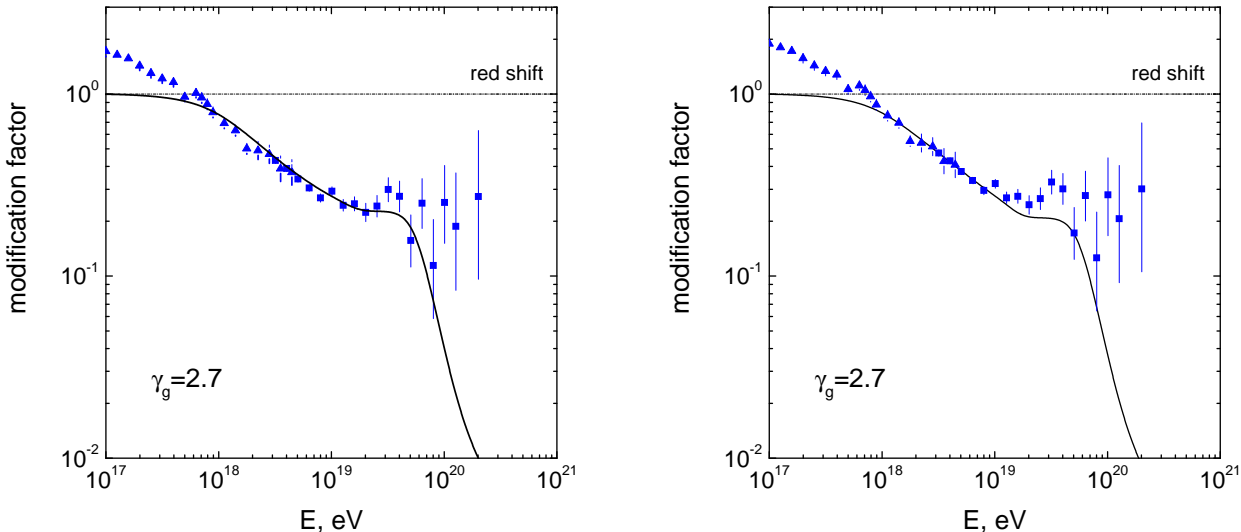


**Fig. 5.** Modification factors for the mixed composition of protons and helium nuclei in comparison with AGASA data. The left panel corresponds to mixing parameter  $\lambda = 0.1$ , and the right panel to  $\lambda = 0.195$ .

rigidity acceleration in single ionized helium gas with mixing parameter  $\lambda = 0.06$  agrees well with the data, and in fully ionized helium gas with  $\lambda = 0.195$  (lower case in Eq. 3) agrees worse. We shall remind that the first and the second ionization potential for helium is very high, 24.6 and 54.4 eV, respectively. In extreme case of neutral helium, the mixed modification factor  $\eta(E) \approx \eta_p(E)$ .  $\Gamma$ -acceleration, and shock acceleration in particular, results in bad agreement of the p+He dip with observations. One should keep in mind the approximate character of our estimates, especially concerning the assumption about power-law spectrum down to  $p_{\min}$ .

If agreement of the proton dip with observations is not accidental (the probability of this is small according to small  $\chi^2/\text{d.o.f.}$ ), Fig 5. should be interpreted as indication to possible acceleration

mechanism. It cannot be shock acceleration, which results in large  $\lambda \propto A^{\gamma_g-1}$ . The large  $\gamma_g$  demands large  $E_{\min}$  in acceleration mechanism to avoid too large cosmic ray luminosity of a source. Correlation with BL Lacs indicates the jet acceleration (see Section 4.).

Another option is given by photodisintegration of UHE nuclei by radiation. The relevant calculations have been recently performed in [27]. It was demonstrated that for the magnetized sources the observed flux above  $1 \times 10^{19}$  eV becomes pure proton one due to photodisintegration by CMB radiation. We can add here that nuclei can be destroyed at lower energies by infra-red radiation inside a source. An example of such model can be given by acceleration in the inner jet, where helium nuclei can be photodisintegrated by infra-red emission from accretion disc.

### 3. Transition from extragalactic to galactic cosmic rays

We will follow this transition going from high to low energies. The critical energy  $E_c \approx 1 \times 10^{18}$  eV is given by the low-energy steepening of the dip (see Fig 1.), below which the more steep galactic spectrum becomes dominant. The data presented in Fig 6. confirm this expectation.

In the left panel the modification factor is shown in comparison with AGASA data (see also Fig 2. for HiRes). At  $E < E_c$  the experimental modification factor exceeds 1, while by definition (see Eq. 1)  $\eta(E) \leq 1$ . It signals about appearance of a new component at  $E < 1 \times 10^{18}$  eV.

In the right panel the spectrum for rectilinear propagation from the sources with different separation  $d$  and with  $\gamma_g = 2.7$  is compared with AGASA data. One can see that at  $E < 1 \times 10^{18}$  eV the calculated extragalactic spectrum becomes less than that observed. In the lower panel the similar

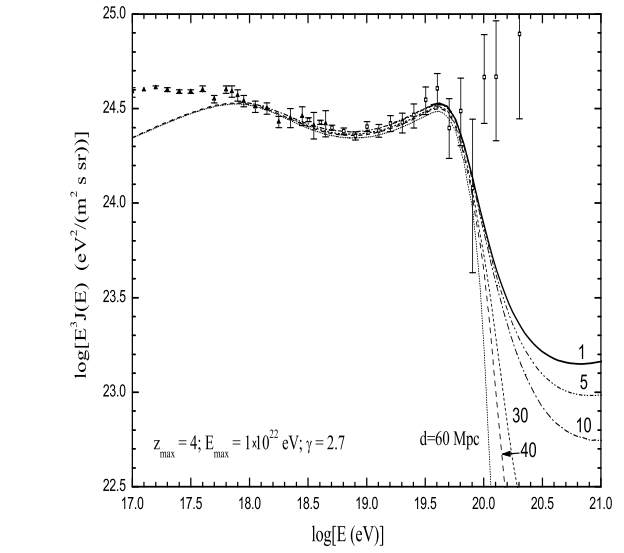
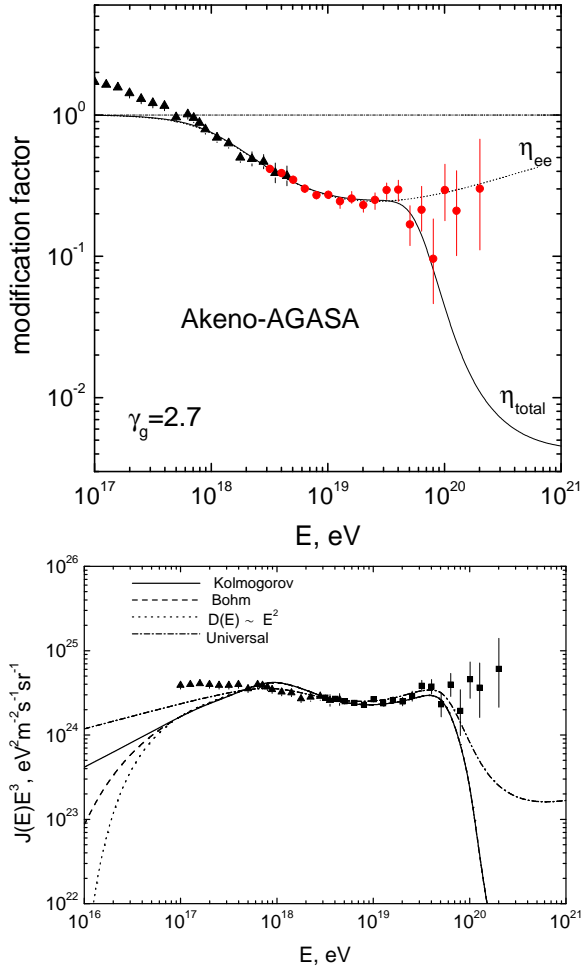


**Fig. 6.** Appearance of transition energy  $E_c \approx 1 \times 10^{18}$  eV in the modification factor compared with AGASA data (left panel), in the spectra for rectilinear propagation for the sources with separation  $d$  indicated in the figure (right panel) and in the spectra for diffusive propagation (lower panel)

comparison is shown for diffusive propagation with different diffusion regimes at lower energies. The dash-dotted curve (universal spectrum) corresponds to the case when the separation between sources  $d \rightarrow 0$ . In all cases the transition again occurs at  $E_c \approx 1 \times 10^{18}$  eV.

What is the reason of this universality?

### 3.1. $E_{\text{eq}}$ , $E_c$ and the second knee $E_{2\text{kn}}$

We study the transition, moving from high towards low energies.  $E_c$  is the beginning of transition (or its end, if one moves from low energies).  $E_c$  is determined by energy  $E_{\text{eq}} = 2.3 \times 10^{18}$  eV, where adiabatic and pair-production energy losses become equal. The quantitative analysis of this connection is given in [18]. We shall give here the semi-quantitative explanation.

The flattening of the spectrum occurs at energies  $E \leq E_c$ , where  $E_c = E_{\text{eq}}/(1 + z_{\text{eff}})^2$  and  $z_{\text{eff}}$  should be estimated as redshift up to which the main contribution to unmodified spectrum occurs. The simplified analytic estimate for  $\gamma_g = 2.6 - 2.8$  gives  $1 + z_{\text{eff}} = 1.5$  and hence  $E_c \approx 1 \times 10^{18}$  eV. In fact, the right and lower panels of Fig 6. presents the exact result of calculations of this kind.

In experimental data the transition is searched for as a feature started at some low energy  $E_{2\text{kn}}$  - the second knee. Its determination depends on experimental procedure, and all what we can predict is  $E_{2\text{kn}} < E_c$ . Determined in different experiments  $E_{2\text{kn}} \sim (0.4 - 0.8) \times 10^{18}$  eV.

The transition at the second knee appears also from consideration of propagation of cosmic rays in the Galaxy (see e.g.[28]).

Being thought of as purely galactic feature, the position of the second knee in our analysis appears as direct consequence of extragalactic proton energy energy losses.

### 3.2. KASCADE data and transition at the ankle

Ankle at energy  $E_a \approx 1 \times 10^{19}$  eV is seen as flattening of the spectrum in data of AGASA, HiRes and Yakutsk detectors in Fig 2. In many works [29] it is considered as a position of transition from galactic to extragalactic cosmic rays (see also [30] for general analysis of the transition). The KASCADE data [31] give a clue for understanding of transition. They confirm the rigidity model, according to which position of a knee for nuclei with charge  $Z$  is connected with the position of the proton knee  $E_p$  as  $E_Z = ZE_p$ . There are two versions of this model. One is the confinement-rigidity model (bending above the knee is due to insufficient confinement in galactic magnetic field), and the other is acceleration-rigidity model ( $E_{\text{max}}$  is determined by rigidity). In both models the heaviest nuclei (iron) start to disappear at  $E > E_{\text{Fe}} = 6.5 \times 10^{16}$  eV. How the gap between  $1 \times 10^{17}$  eV and  $1 \times 10^{19}$  eV is filled?

Protons start to disappear at  $E > 2.5 \times 10^{15}$  eV. Where they came from at  $E > 1 \times 10^{17}$  eV to be seen in the Akeno detector?

To ameliorate these problems, the authors of [29] shift the ankle to  $3 \times 10^{18}$  eV or assume another galactic component, which appears after the iron knee. The second-knee model suggests a solution as transition (being completed) at  $E_c \approx 1 \times 10^{18}$  eV.

The ankle model needs acceleration by galactic sources up to  $1 \times 10^{19}$  eV (at least for iron nuclei). The second knee model ameliorates this requirement by one order of magnitude.

The second-knee model predicts the spectrum shape down to  $1 \times 10^{18}$  eV with extremely good accuracy ( $\chi^2/\text{d.o.f.} = 1.12$  for Akeno-AGASA and  $\chi^2/\text{d.o.f.} = 0.908$  for HiRes). In the ankle model one has to consider this agreement as accidental, though such hypothesis has very small probability, determined by  $\chi^2$  cited above.

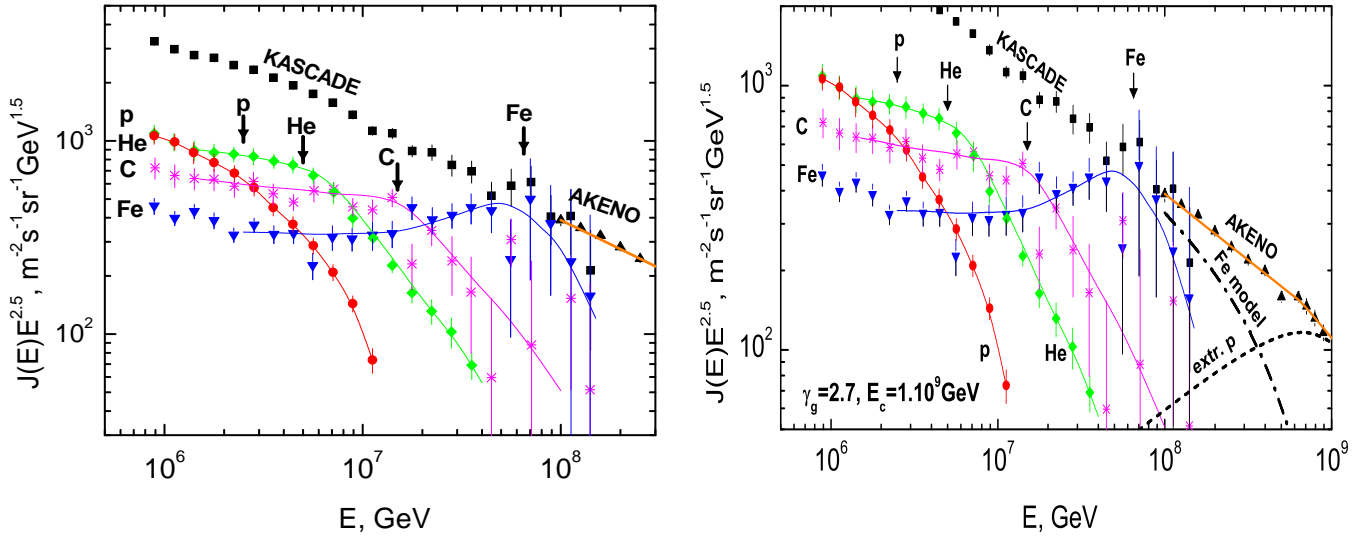


**Fig. 7.** In the *left panel* the proton and nuclei spectra are shown according to KASCADE data. The arrows labelled by p, He, C and Fe show the positions of corresponding knees, calculated as  $E_Z = ZE_p$ , with  $E_p = 2.5 \times 10^6$  GeV (the proton knee). One can notice the agreement between calculated and observed positions of the knees. In the *right panel* one can see the extragalactic proton spectrum, calculated in AGN model (see Section 4.), and galactic iron-nuclei spectrum (Fe-model) predicted by this model.

### 3.3. Comparison of the dip and ankle transitions

*Dip transition* is based on rigidity model for galactic cosmic rays, according to which the proton knee is at  $E_p \approx 2.5 \times 10^{15}$  eV and iron knee is at  $E_{Fe} = ZE_p \approx 6.5 \times 10^{16}$  eV. At  $E > E_{Fe}$  the galactic spectrum is predicted to have steepening. The physical spectra predicted in the rigidity model are those for different nuclei, while the sum of these spectra has no direct physical meaning. The total spectrum between  $E_p$  and  $E_{Fe}$  must show some oscillations due to the knees of the different nuclei, and the power-law *total* spectrum  $E^{-\gamma}$  at  $E_p \leq E \leq E_{Fe}$  is nothing more than a fit, which cannot be extrapolated beyond  $E_{Fe}$ . The question whether or not continuation of  $E^{-\gamma}$  spectrum at  $E > E_{Fe}$  fits the flux measured at  $E > E_c = 1 \times 10^{18}$  eV is unphysical within this model.

The maximum acceleration energy  $E_{\max}$  for galactic cosmic rays may be in this model  $E_{\max} < 1 \times 10^{18}$  eV for iron nuclei, which fits SN shock acceleration models.

At  $E > E_{Fe}$  the galactic iron flux steepens, while extragalactic flux flattens at energies below  $E_c = 1 \times 10^{18}$  eV (see curves 'Fe-model' and "extr. p" in the right panel of Fig 7.). These two curves thus inevitably intersect at some energy  $E_{tr}$ , providing the transition. The energy behaviour of both curves and value of  $E_{tr}$  are model dependent.

In Fig 7. (right panel) the transition is shown for the model described in Section 4. The transition is characterised by three energies  $E_{Fe} \approx 6.5 \times 10^{16}$  eV,  $E_{tr} \approx 4 \times 10^{17}$  eV and  $E_c \approx 1 \times 10^{18}$  eV, and by fluxes  $J_{\text{gal}}(E_{Fe}) \approx 1.8 \times 10^{-17} \text{ m}^{-2}\text{s}^{-1}\text{sr}^{-1}\text{GeV}^{-1}$  and  $J_{\text{extr}}(E_c) \approx 3.2 \times 10^{-21} \text{ m}^{-2}\text{s}^{-1}\text{sr}^{-1}\text{GeV}^{-1}$ . It is difficult to find any fine-tuning in these values. The flux at the 'end' of galactic spectrum,  $E_{Fe}$ , and the flux at the starting of extragalactic part of the spectrum,  $E_c$ , differ by 4 orders of magnitude, and thus there is no conspiracy between these two values.

The structure of the second knee, composed by galactic iron and extragalactic protons (see right panel in Fig 7.), is very similar to the structures of the other knees: there is a sharp transition from galactic iron to extragalactic protons (similar to transitions between different galactic nuclei), which in both cases results in the total spectrum with a faint transition feature.

The predicted spectrum shape above the second knee ( $1 \times 10^{18} - 4 \times 10^{19}$  eV) is model inde-

pendent and is confirmed by observations. The ankle at  $E_a \sim 1 \times 10^{19}$  eV appears automatically in the calculations as the part of the dip.

The *ankle model* is based on the assumption that transition occurs at ankle  $E_a \sim 1 \times 10^{19}$  eV, where experimental data show flattening of the spectrum. An advantage of this model is given by flatter generation spectrum ( $\propto E^{-2.3}$ ), which allows to diminish the source luminosities. The disadvantages are connected with models for galactic cosmic rays at  $E \lesssim 1 \times 10^{19}$  eV. What particles fill the gap between the iron knee  $E_{\text{Fe}} \approx 6.5 \times 10^{16}$  eV and the ankle  $E_a \sim 1 \times 10^{19}$  eV? If they are iron nuclei, why they have the same spectrum as the *sum* of different nuclei at  $E < E_{\text{Fe}}$ ? How protons, which start to disappear above the proton knee  $E_p \approx 2.5 \times 10^{15}$  eV re-appear again at energy  $E > 1 \times 10^{17}$  eV comprising about 10 % of the Akeno flux? Why the spectrum at  $1 \times 10^{18} \leq E \leq 4 \times 10^{19}$  eV has the dip feature explained so well by extragalactic protons?

#### 4. The AGN model

The AGN as sources of UHECR meet the necessary requirements: (i) to provide the necessary energy output, (ii) to have the space density  $n_s \sim (1 - 3) \times 10^{-5} \text{ Mpc}^{-3}$  necessary for the observed small-scale anisotropy [32] and (iii) to provide the observed correlations with BL Lacs [33].

##### Acceleration

According to the AGN unified model BL Lacs are Fanaroff-Riley galaxies with jets in the direction of the observer. Thus, correlations of UHECR particles with BL Lacs imply the jet acceleration of the particles. Acceleration in the jets due to pinch mechanism was suggested first for tokamaks (where it was confirmed on the laboratory scale) and then was rescaled in [34] to cosmic sizes. The

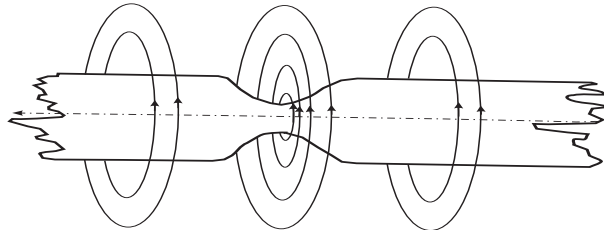


**Fig. 8.** Pinch-neck instability in jet

pinch mechanism of acceleration works due to pinch-neck instabilities, illustrated in Fig 8., which are accompanied by production of strong electric field. The solution of kinetic equations [34] gives the power-law spectrum of accelerated particles  $q(E) \propto E^{-\gamma_g}$  with  $\gamma_g = 1 + \sqrt{3}$ , which is practically the same as in our calculations. The maximum energy of acceleration can well exceed  $10^{20}$  eV, if to rescale the laboratory pinch scale, where MeV energies were observed, to the AGN size.

##### Generation spectrum and source luminosity

Inspired by the pinch acceleration mechanism, we assume ad hoc the generation spectrum in the form:

$$q_{\text{gen}}(E) \propto \begin{cases} E_g^{-2} & \text{at } E_g \leq E_c \\ E_g^{-2.7} & \text{at } E_g \geq E_c, \end{cases} \quad (6)$$

with  $E_c$  being a free parameter and with the maximum acceleration energy  $E_{\text{max}} = 1 \times 10^{21}$  eV. For  $E_c \sim 1 \times 10^{18}$  eV the *emissivity* needed to fit the calculations to the AGASA flux is  $\mathcal{L}_0 =$

$3.5 \times 10^{46}$  erg/yr Mpc<sup>3</sup>. With space density of the sources taken from small-angle clustering  $n_s \sim 3 \times 10^{-5}$  Mpc<sup>-3</sup>, the luminosity of a source is  $L_p = 3.7 \times 10^{43}$  erg/s, which is quite low for AGN.

With these assumptions the calculated spectra in comparison with observations are shown in Fig 9. The AGASA excess, if real, needs for its explanation another component. shown by dashed line in the AGASA panel (e.g. from superheavy dark matter [35]).

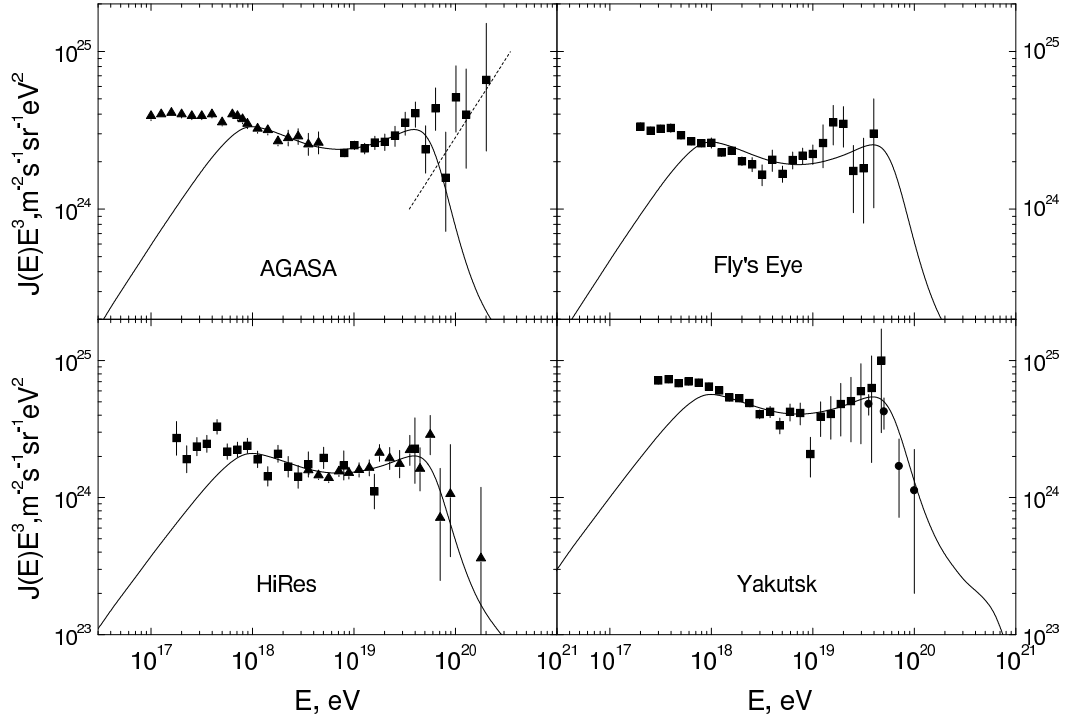


**Fig. 9.** The AGN-model predicted spectra compared with data.

### Transition from extragalactic to galactic cosmic rays

Assuming that galactic cosmic rays at  $E > 1 \times 10^{17}$  eV are dominated by iron nuclei, we calculate this flux subtracting the extragalactic proton flux, calculated in AGN model, from the measured Akeno flux. The result is shown in Fig 7. (right panel).

## 5. Conclusions

1. The *dip* is the spectrum feature produced by interaction of UHE extragalactic protons with CMB radiation. In terms of modification factor it is practically model-independent, depending weakly on generation index  $\gamma_g$ , mode of propagation (rectilinear or diffusive propagation), discreteness and inhomogeneity in source distribution, local overdensity or deficit of the sources, maximum acceleration energy and fluctuations in energy losses. For non-evolutionary sources, when the number of free parameters is minimal ( $\gamma_g$  and total flux normalization) the agreement with observational data of Akeno-AGASA, HiRes, Fly's Eye and Yakutsk (see Fig 2.) is very good and characterised by  $\chi^2/d.o.f.$  equal to 1.12 for Akeno-AGASA and 0.908 for HiRes. It implies very low probability of accidental agreement. *This is the strong evidence that majority of primaries observed at  $1 \times 10^{18} - 4 \times 10^{19}$  eV are extragalactic protons propagating through CMB.*
2. The dip is modified by evolution of the sources and by presence of extragalactic nuclei as the

primaries. The latter effect points to some acceleration mechanism or to the sources, where He-nuclei are photodisintegrated (see Section 2.).

3. The dip has two flattenings, at low energy  $E_c \approx 1 \times 10^{18}$  eV and at high energy  $E_a \approx 1 \times 10^{19}$  eV. The latter, *ankle*, is confirmed in most observations (see Fig 2.). The former provides the dominance of more steep galactic component at  $E < E_c$ . There are three evidences of the transition from extragalactic to galactic cosmic rays at energy  $E_c$  shown in Fig 6. The observed transition should be seen at energy  $E < E_c$ , and this feature is observed as the *second knee*. The energy  $E_c$ , where transition from *galactic to extragalactic* cosmic rays is completed, is directly connected with energy  $E_{\text{eq}}$ , where adiabatic and pair production energy losses for extragalactic protons are equal.

4. The transition from galactic to extragalactic cosmic rays at the ankle is discussed in subsections 3.2. and 3.3. For the ankle transition one must assume that agreement of the dip with observations is accidental, while in case of the dip the ankle is an automatic feature (part of the dip).

5. The above-listed conclusions are valid for model-independent analysis with basically two assumptions: the proton spectrum is power-law at  $E \gtrsim 1 \times 10^{18}$  eV and sources are distributed uniformly with arbitrary separation  $d$ . The AGN model described in Section 4. uses some specific generation spectrum, inspired by pinch acceleration mechanism. This model explains small-scale anisotropy and correlations with BL Lacs, predicts spectra of UHECR measured in Akeno-AGASA, HiRes, Fly's Eye and Yakutsk experiments and quantitatively describes the transition from extragalactic to galactic cosmic rays at the second knee. The latter is quite similar to transitions from one type of nuclei to another in the first knee.

## Acknowledgements

I am grateful to Roberto Aloisio, Pasquale Blasi, Askhat Gazizov and Svetlana Grigorieva for most efficient and pleasant joint work, which results are (preliminary) presented here. We thank Transnational Access to Research Infrastructure ILIAS-TARI through the contract HPRI-CT-2001-00149 within which most of work presented here has been performed. I am grateful to Vladimir Ptuskin, Oleg Smirnov and Alan Watson for valuable discussions.

## References

- [1] K. Greisen, Phys. Rev. Lett. **16**, 748 (1966);  
G. T. Zatsepin, V.A. Kuzmin, Pisma Zh. Experim. Theor. Phys. **4**, 114 (1966).
- [2] C. T. Hill and D. N. Schramm, Phys. Rev. D **31**, 564 (1985).
- [3] V. S. Berezinsky and S. I. Grigorieva, Astron. Astroph. **199**, 1 (1988).
- [4] S. Yoshida and M. Teshima, Progr. Theor. Phys. **89**, 833 (1993).
- [5] T. Stanev et al., Phys. Rev. D **62**, 093005 (2000).
- [6] V. Berezinsky, A. Z. Gazizov, S. I. Grigorieva, hep-ph/0204357.
- [7] V. Berezinsky, A. Z. Gazizov, S. I. Grigorieva, astro-ph/0210095.
- [8] V. Berezinsky, A. Z. Gazizov, S. I. Grigorieva, Proc. of Int. Workshop "Extremely High-Energy Cosmic Rays" (eds M.Teshima and T. Ebisuzaki), Universal Press, Tokyo, Japan, p. 63 (2002).
- [9] V. Berezinsky, A. Z. Gazizov, S. I. Grigorieva, Phys. Lett. B **612**, 147 (2005) [astro-ph/0502550].
- [10] K. Shinozaki and M. Teshima, Nucl. Phys. B (Proc. Suppl.) **136**, 18 (2004).
- [11] HiRes collaboration, Phys. Rev. Lett. **92**, 151101 (2004).

- [12] D. J. Bird *et al.* [Fly's Eye collaboration], Ap. J. **424**, 491 (1994).
- [13] A. V. Glushkov *et al.* [Yakutsk collaboration] Proc. of 28th Int. Cosmic Ray Conf. (Tsukuba, Japan), **1**, 389 (2003);
- [14] M. Ave *et al.* [Haverah Park collaboration], Astrop. Phys. **19**, 61 (2003).
- [15] M. Nagano and A. Watson, Rev. Mod. Phys. **72**, 689 (2000).
- [16] R. Aloisio and V. Berezinsky, Astroph. J. **612**, 900 (2004).
- [17] M. Lemoine, Phys. Rev. D **71**, 083007 (2005).
- [18] R. Aloisio and V. Berezinsky, Astroph. J. **625**, 249 (2005).
- [19] G. Archbold and P. V. Sokolsky, Proc. of 28th ICRC, 405 (2003).
- [20] T. Abu-Zayyad *et al.*, Phys. Rev. Lett. **84**, 4276 (2003).
- [21] A. V. Glushkov *et al.* (Yakutsk collaboration) JETP Lett. **71**, 97 (2000).
- [22] M. Honda *et al.* [Akeno collaboration], Phys. Rev. Lett. **70**, 525 (1993).
- [23] A. Watson, Nucl. Phys. B (Proc. Suppl.) **136**, 290 (2004).
- [24] The Pierre Auger Collaboration, astro-ph/0507150 (2005).
- [25] D. De Marco, P. Blasi, A. Olinto, astro-ph/0507324 (2005).
- [26] D. Allard *et al.*, astro-ph/0505566 (2005).
- [27] G. Sigl and E. Armengaud, astro-ph/0507656 (2005).
- [28] P. Biermann *et al.*, astro-ph/0302201 (2005); J. R. Hoerandel, Astrop. Phys. **19**, 193 (2003); S. D. Wick, C. D. Dermer, A. Atoyan, Astropart. Phys. **21**, 125 (2004).
- [29] A. M. Hillas, Nucl. Phys. B (Proc. Suppl.) **136**, 139 (2004); E. Waxman, Phys. Rev. Lett. **75**, 386 (1995); M. Vietri, Astroph. J. **453**, 883 (1995); T. Wibig, A. W. Wolfendale, J. Phys. G **31**, 255 (2005); D. Allard *et al.*, astro-ph/0505566 (2005).
- [30] D. De Marco, T. Stanev, astro-ph/0506318 (2005)
- [31] K.-H. Kampert *et al.* (KASCADE-Collaboration), Proceedings of 27th ICRC, volume "Invited, Rapporteur, and Highlight papers of ICRC", 240 (2001).
- [32] P. Blasi, D. De Marco, Astropart. Phys. **20**, 559 (2004); M. Kachelriess, D. Semikoz, Astropart. Phys. **23**, 486 (2005).
- [33] P. G. Tinyakov and I. I. Tkachev, JETP Lett. **74**, 445 (2001).
- [34] V. P. Vlasov, S. K. Zhdanov, B. A. Trubnikov, Soviet Physics of Plasma **16**, 1457 (1990).
- [35] V. Berezinsky and M. Kachelriess, Phys. Rev. D **63** 034007 (2001); R. Aloisio, V. Berezinsky, M. Kachelriess, Phys. Rev. D **69**, 094023 (2004).